Co-detection: Ultra-reliable Nanoparticle-Based Electrical Detection of Biomolecules in the Presence of Large Background Interference

Yang Liu,[1] Evangelyn C. Alocilja[2], Shantanu Chakrabartty,[1*]

[1]Department of Electrical and Computer Engineering, Michigan State University, 2120 Engineering Building, East Lansing, MI 48824, USA

[2]Department of Biosystems and Agricultural Engineering, Michigan Sate University 115 Farell Hall, East Lansing, MI 48824, USA

[*]To whom correspondence should be addressed. E-mail: shantanu@egr.msu.edu

Abstract:

Contrary to popular belief, we report that background interference in conductimetric biochips can be exploited using a novel "co-detection" principle to significantly improve the reliability of detecting trace quantities of biomolecules. The technique called "co-detection" exploits the non-linear redundancy amongst synthetically patterned biomolecular logic circuits for deciphering the presence or absence of target biomolecules in a sample. In this paper, we demonstrate the "co-detection" principle on gold-nanoparticle based conductimetric soft-logic circuits which uses a silver-enhancement technique for signal amplification. Using co-detection, we have been able to measure a 1000 times improvement in the reliability of detecting mouse IgG at concentration levels that are 10^5 lower than the concentration of rabbit IgG which serves as background interference.

Description

A major challenge in the area of biosensors is to be able to detect target biomolecules in the presence of large background interference[1]. In many cases, background interference could simply constitute the presence of non-target analytes which could not only produce non-specific binding events but also cause steric hindrance, preventing binding between target analytes with its specific recognition probes (antibody or DNA)[2]. Most of the reported methods in biosensors either aim to reduce the effect of background interference using pre-filtering techniques[3] or aim to boost the concentration of the target analyte using pre-concentration[4] or target-amplification (e.g. polymerase chain reaction or PCR)[5-6]. In this paper we report that background interference created by the presence of non-specific analytes can be exploited to amplify and improve the reliability of detection of the target analyte. The principle which we call "co-detection" can simply be illustrated using a biosensor reliability curve in **Fig. 1a** where analyte 1 serves as the target to be detected and analyte 2 serves as the background interference. Ideally, the detection error-rate (DER) or the sum of false-positive or false-negative errors decreases with the increase in analyte 1 concentration (ignoring the Hook effect[7]) and the DER is largely unaffected or increases when the concentration of analyte 2 (acting as background interference) increases. However in "co-detection", addition of analyte 2 reduces the DER for analyte 1, as illustrated in **Fig. 1a**, and hence enhances the reliability of detection.

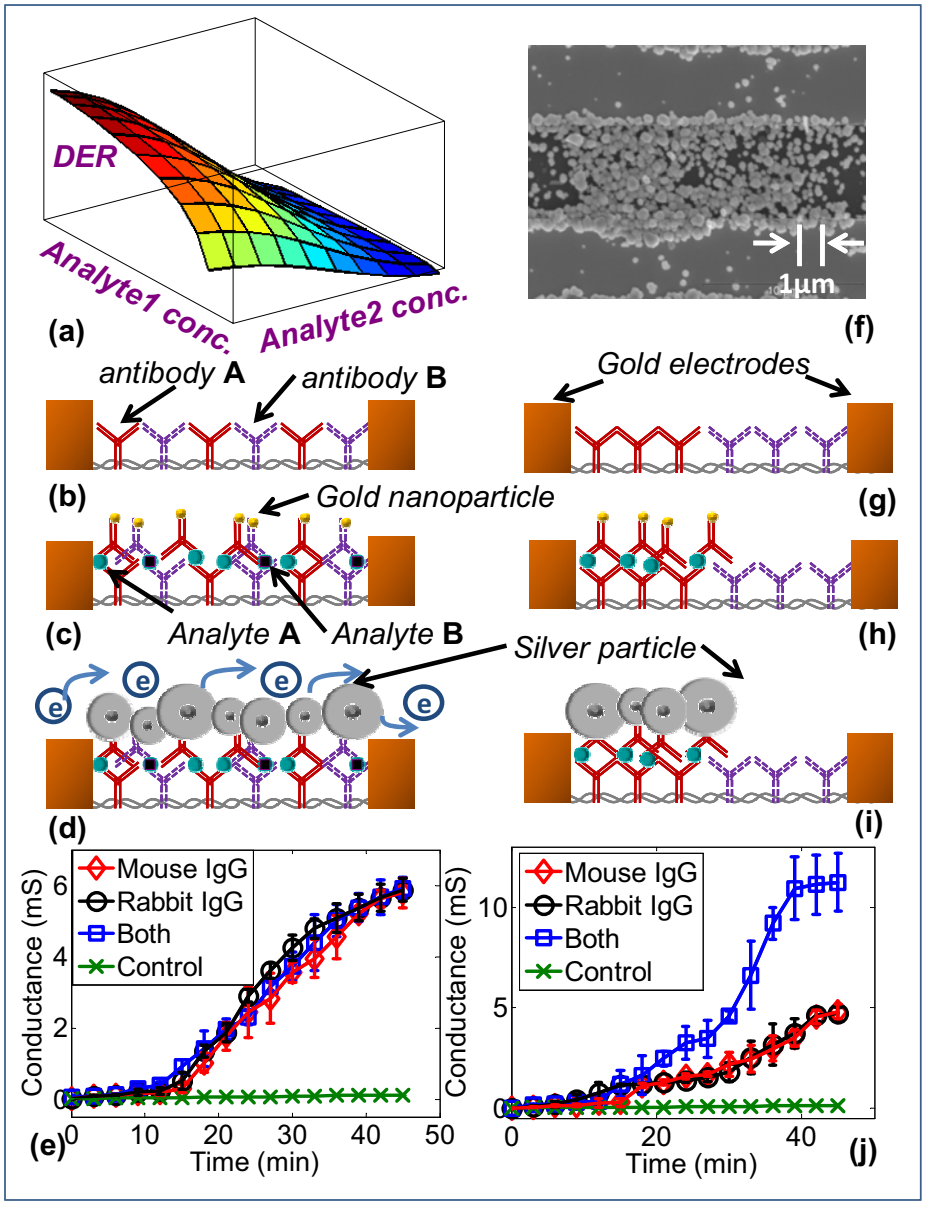

Fig. 1. *(a) Illustration of "co-detection" principle, where the presence of analyte2 enhances the reliability of detection of analyte1; (b) architecture of an OR gate where the anti-mouse IgG and anti-rabbit IgG are mixed and patterned between the electrodes; (c) formation of a sandwich assay between the target analyte, its specific antibody and a secondary antibody conjugated with gold nanoparticle; (d) silver-enhancement procedure where the gold nanoparticle catalyzes the silver which deposits around the particle, thus increasing its size and in the process forming a conductive bridge between the electrodes; (e) conductance measured across the electrodes of the OR gate during the enhancement procedure for different logic conditions; (f) SEM image of the inter-electrode spacing showing the formation of the conductive bridge by silver enhanced gold nanoparticle; (g) architecture of an AND gate where the anti-mouse IgG and anti-rabbit IgG are cascaded between the electrodes; (h)&(i) formation of partial sandwich assay and conductive bridge due to the presence of only one of the analyte; (j) conductance measured across the electrodes of the AND gate during the silver-enhancement procedure under different logic conditions.*

Co-detection is similar in spirit to many noise exploitation techniques like stochastic resonance which has been reported in physics[8] and biology[9-10], where it has been shown that the addition of random noise into a non-linear system in fact improves the system sensitivity. However, the key towards implementing co-detection in biosensors is to effectively control the coupling (or interference) between different analytes and to exploit the non-linear response of the biosensor. In this regard, we had previously proposed a forward error correction (FEC) immunosensor[11] platform where biomolecular soft-logic circuits were fabricated to synthetically produce interference between the binding events of multiple pathogens. In this work, we first report the fabrication of biomolecular logic circuits using silver enhanced nanoparticles and then use the biosensor platform to demonstrate the "co-detection" principle. We show that the proposed approach can improve the reliability of detecting target analyte (mouse IgG) by three orders of magnitude when the background interference (rabbit IgG concentration) is more than 10^5 higher than the target analyte (mouse IgG) concentration.

The architecture of the two logic functions (soft-AND and soft-OR) which has been used in this work is shown in **Fig. 1b** and **Fig. 1g** where antibodies corresponding to analyte A and B (mouse IgG and rabbit IgG) are patterned at different spatial locations between two gold electrodes. For the soft-OR logic gate, a mixture of goat anti-rabbit IgG and goat anti-mouse IgG was patterned as shown in **Fig. 1b**, where as for the soft-AND gate, the antibodies were patterned in a cascaded fashion as shown in **Fig. 1g** (**Supplementary Fig. 1**).

When the analyte is applied to the immobilized biochips, the target biomolecules (mouse and rabbit IgG) hybridize with their specific antibodies. The secondary antibodies conjugated with gold (Au) nanoparticles are then applied to the biochip, which leads to the formation of a sandwich assay as shown in **Fig. 1c**. In this stage, the current measured between the electrodes (for a fixed potential difference) is small. The next step involves a silver enhancement technique to amplify the hybridization events into a measurable electrical signal. The sandwich assay is exposed to a solution of Ag(I) and hydroquinone (photographic developing solution). The gold nanoparticles act as a catalyst and reduce silver ions into metallic silver in the presence of a reducing agent (hydroquinone). The reduced silver then deposits on the gold surface, thus enlarging the size of the gold nanoparticles as shown in **Fig. 1d**. As the size of the silver islands grows, they provide shorter paths for electrons to hop between the electrodes. With the increase in enhancement time (the time of the exposure with the silver enhancer solution), the consistent growth of silver-enhanced particles completely bridges the area between the electrodes (shown in **Fig. 1d**). Even though, silver-enhancement technique has been used for conductometric DNA arrays and immunoasssays[13-17], it has not been yet extended to implement logic-functions as is reported in this work. In the case of the soft-OR gate the conductive bridge between the electrodes is formed when either one of the analytes (rabbit IgG or mouse IgG) is present in the sample, assuming that the density of antibody probes is large enough. This scenario is shown in **Fig. 1d** for the case when both rabbit IgG and mouse IgG are present in the sample and **Fig. 1f** shows an SEM verification of the bridge formation between the two electrodes. **Fig. 1e** shows the measured conductance across the electrodes during the process of silver enhancement under

different logic conditions (control, only mouse IgG present, only rabbit IgG present and both mouse and rabbit IgG present). The figure shows that indeed compared to the control experiment, the conductance change is significantly large for all the logic conditions and increases with increase in enhancement time.

In the case of ideal AND gate (shown in **Fig. 1g**), the bridge across the electrode will be completely formed only when both of biomolecules (rabbit IgG and mouse IgG) are present. However, for a soft-AND gate, the bridge can be partially formed (shown in **Fig. 1h and Fig. 1i**) when only one of the analytes is present. This leads a smaller conductance change compared to the completely formed bridge. **Fig. 1j** shows the conductance measured across the electrodes of the AND gate under different logic conditions (control, only one analyte present and both analyte present). The result shows that the change in conductance is the largest when both of biomolecules are present as compared to the condition when only one of the biomolecule is present, thus verifying the soft-AND logic function. Also, similar to the OR gate response, the conductance increases with increase in enhancement time.

We have also verified that the responses of the fabricated soft-AND and soft-OR gates are consistent across different concentrations of the input analytes. **Fig. 2a** and **Fig. 2b** show the conductance measured across both the gates for different concentrations of analytes and under different logic conditions. For this experiment, the rabbit IgG and mouse IgG were serially diluted using PBS to prepare 100-fold dilutions representing IgG concentrations ranging from 12 μg/mL-0.12 ng/mL. Each of the tests was repeated three times and the results were measured every 3 minutes after the replacement of new silver enhancer solution onto biochips. “Control” experiments for all the experiments were

obtained using bovine IgG. It can be seen from **Fig. 2a** and **Fig. 2b** that under different concentration levels of analytes the response of the logic function remains consistent, however, the magnitude of the measured conductance scales log-linearly with concentration. The measured data was then used to estimate the parameters of a two-dimensional coupled log-linear model[18], one for each of the logic gates as shown in **Fig. 2e** and **Fig. 2f** (**Supplementary Fig. 3 and Supplementary Table 1**). Also included in the set of models were single analyte biochips whose measured conductance was only dependent on the concentration of a single analyte (experimental results shown in **Fig. 2c** and **Fig. 2d**). The responses of the single analyte biochips are shown in **Fig. 2g** and **Fig. 2h** which are one-dimensional log-linear models.

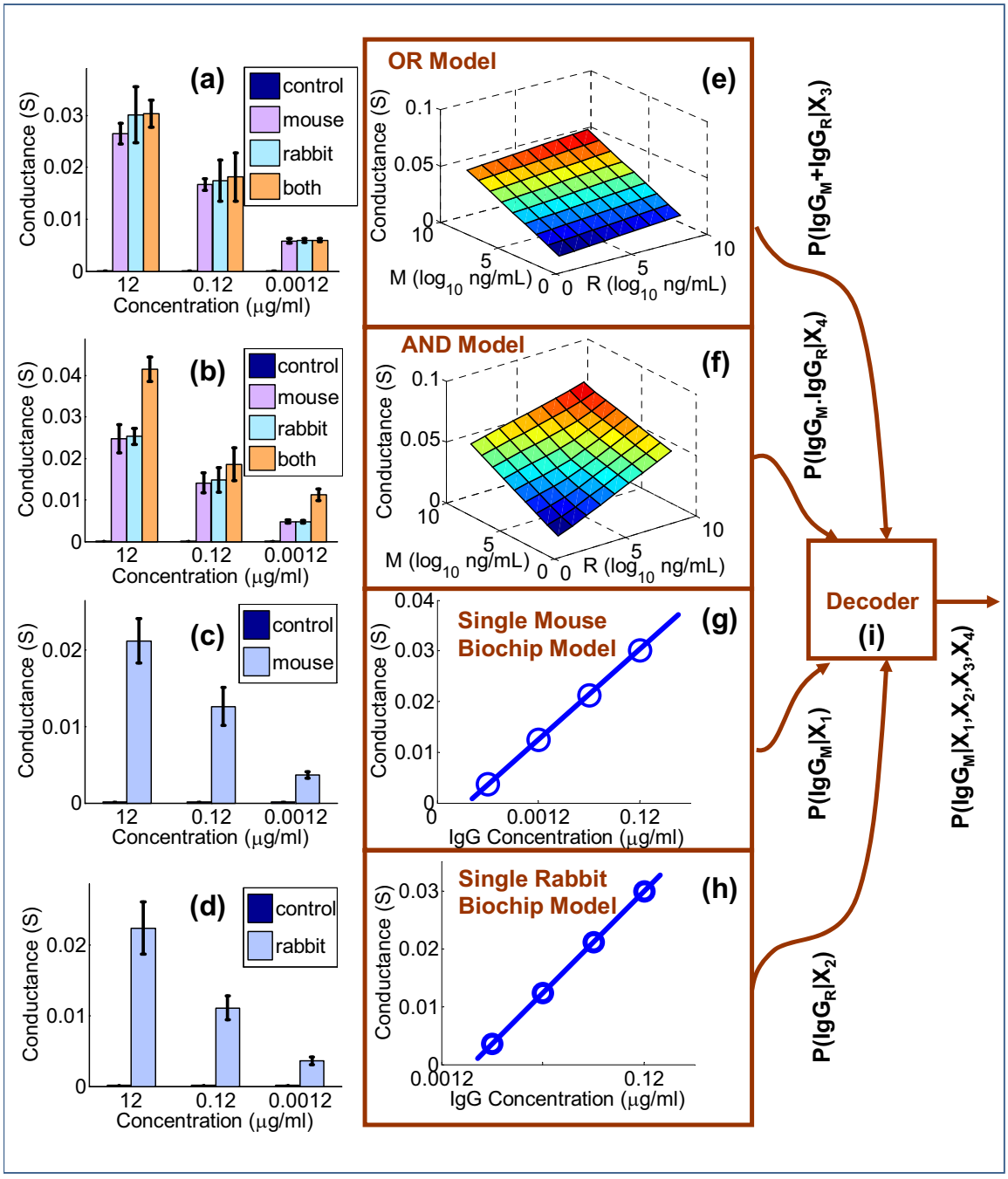

Fig. 2. *Experimental results showing the measured conductance from (a) a soft-OR logic gate for different concentration levels of rabbit and mouse IgG; (b) a soft-AND logic gate for different concentration levels of rabbit and mouse IgG; (c) a mouse IgG specific biochip for different concentration levels of mouse IgG; (d) a rabbit IgG specific biochip for different concentration levels of rabbit IgG; coupled log-linear models determined using experimental data for (e) soft-OR logic-gate; (f) soft-AND logic-gate; (g) mouse IgG biochip; (h) rabbit IgG biochip; (i) architecture of the Bayesian decoder used to compute the posterior probability of the presence of mouse IgG given an array of conductance measurements.*

To demonstrate the "co-detection'' principle, a total of six different biochips were used: two single analyte biochip specific to mouse IgG, two single analyte biochips specific to rabbit IgG, one soft-AND biochip and one soft-OR biochip. The experimental procedure involved the following steps: (a) an unknown sample (containing different concentration of mouse and rabbit IgG) were applied to the six biochips; (b) the measured conductance X_i were presented as inputs to the biosensor model, whose outputs were normalized to generate posterior probabilities. For example, the soft-OR biochip model (**Fig. 2a**) generated the posterior probability $P(IgG_M + IgG_R|X_i)$ that either one of the analytes (rabbit or mouse IgG) is present given the conductance measurement X_i. As shown in **Fig. 2i**, all the posterior probabilities are combined together using Bayesian techniques to compute the probability of presence of target analytes $P(IgG_M|X_1,..,X_6)$, $P(IgG_R|X_1,..,X_6)$ given all the measured conductances $X_1,..,X_6$ (from six biochips) (The decoder is described in **Supplementary Fig. 4-5**) The probability scores are compared against a pre-determined threshold to make a positive identification of the target analyte. **Fig. 3a-b** shows the detection error rate (false positive error and false negative error) curves that were obtained by Monte-Carlo simulations using the biochip behavioral models. For this experiment, the magnitude of noise was estimated from the experimentally determined error bars as shown in **Fig. 2a-d**. In **Fig. 3a**, the concentration of rabbit IgG is increased which as expected leads to the decrease in its DER. However, the increase in concentration of mouse IgG also leads to the decrease in DER, clearly indicating the "co-detection" principle. A similar behavior was also observed for the DER of mouse IgG as shown in **Fig. 3b**. For comparison purposes, **Fig. 3c** shows the DER curves that were obtained if six independent rabbit and mouse IgG biochips are

used for detection. This scenario replicates the testing strategy commonly employed in diagnostics where repeated experiments followed by majority voting are performed to obtain reliable detection results. The plots in **Fig. 3c** clearly show the absence of "co-detection" which is expected as there is very little coupling between different detection tests.

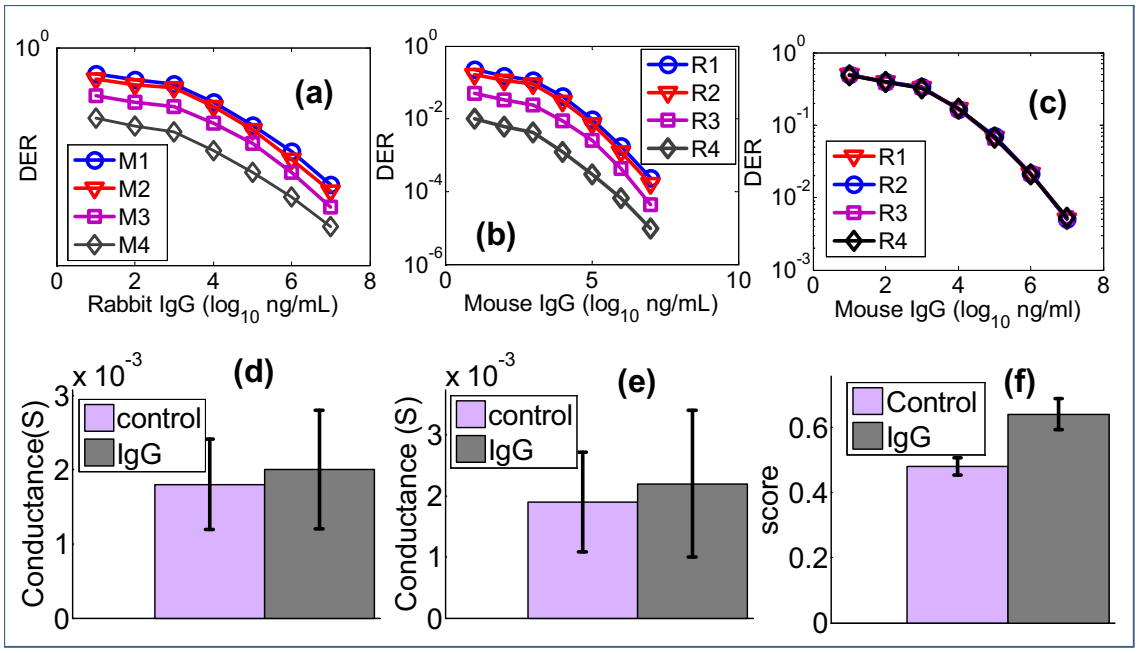

Fig. 3. *Demonstration of "co-detection" principle based on mouse IgG experiments and behavioral simulations. Detection error-rate (DER) curves obtained using behavioral models in Fig. 2 for different concentration of rabbit and mouse IgG: (a) showing co-detection when presence of higher concentration of mouse IgG enhances the detection reliability of rabbit IgG. M1 represents mouse IgG concentration: 1 ng/mL; M2 represents mouse IgG concentration: 100 ng/mL; M3 represents mouse IgG concentration: 10 ug/mL; M4 represents mouse IgG concentration: 1 mg/mL. (b) presence of higher concentration of rabbit IgG enhances the detection reliability of mouse IgG; R1-R4 hold similar meaning and same value as M1-M4. (c) absence of co-detection in the conventional repetitive tests where rabbit IgG does not affect the detection reliability of mouse IgG; Experimental verification of co-detection: (d) results from a mouse IgG biochip when 100pg/ml mouse IgG is used; (e) results from a mouse IgG biochip when 100pg/ml mouse IgG is used in presence of 10μg/ml of rabbit IgG; (f) results from the Bayesian decoder showing significant improvement in reliability of mouse IgG detection in the presence of background rabbit IgG.*

We now report results where the "co-detection" principle has been experimentally verified in the detection of mouse IgG. For the experiment, 100 pg/mL mouse IgG is added to the solution of 10 ug/mL rabbit IgG which serves as the background interference. 10 μg/mL bovine IgG is used as negative control experiment. For calibration purposes, we first applied a sample containing only 100 pg/mL mouse IgG to a single mouse IgG biochip. **Fig. 3d** shows the detection result compared against the negative control. Even though the experiments show that on average the silver-enhancement technique can detect the trace quantity of mouse IgG, the variance of the experiment (shown by the overlap between the error bars) is too large for reliable confirmation. **Fig. 3e** shows the result obtained from the single analyte biochip when a mixture of 100 pg/mL mouse IgG and 10 μg/mL rabbit IgG is applied. As expected, the results show similar response as the previous experiment since anti-mouse IgG are non-specific to rabbit IgG. In the last set of experiment, the mixture with similar composition was applied to the six biochips and the measured conductances were process by the decoding algorithm. **Fig. 3f** shows the response obtained from the decoder and compares it with results obtained for the negative control experiments. Note that the output of the decoder is the normalized score indicating the presence or absence of mouse IgG. It can be clearly seen that not only has the magnitude of the scores have increased significantly compared to the control, the variance of the results have also decreased by orders of magnitude. Since there is no overlap between error bars, perfect detection of mouse IgG can be achieved in the presence of high background concentration of rabbit IgG. We believe that the non-linear response of the FEC biochip in conjunction with "co-detection" is the primary reason behind the improvement in reliability. The presence of large background interferences

introduces conduction sites which can be easily populated by the target analytes. The computational approach for co-detection bears similarity to DNA signature discovery techniques[19]. However, the key difference in this work is exploitation of background noise instead of suppressing it. We would also like to point out that even though in our report, we have used only two analytes (mouse IgG and rabbit IgG) to demonstrate the "co-detection" principle, the approach is generic and can be extended to any kinds and any number of analytes. In fact we anticipate significant improvements in reliability as the number of analytes increases. This is because of the exponential increase in the side-information that is available through coupling between multiple binding events. One of the key applications where "co-detection" could be used in the future is in the early diagnosis of HIV. Early diagnosis of HIV requires detecting trace quantity of HIV biomolecules that are usually accompanied by other non-specific biomolecules that directly interfere in the detection process[20] and hence require a long-time for confirmation tests. The improvement in reliability offered by "co-detection" will reduce the window period for positive or negative diagnosis and hence can facilitate rapid screening.

Methods

Biochip fabrication

The following procedure was used for fabricating the silver-enhanced gold nanoparticle based biochip and then immobilizing specific antibodies onto the substrate. The biochips were fabricated from 400 silicon wafers (p-type 100, thickness 500-550 μm). A 2 μm thick layer of thermal oxide was grown over the silicon to serve as an insulator between

the electrodes and the substrate. Photolithography was used to pattern photo-resist (PR) followed by deposition of metal electrodes through evaporation of 10nm of chrome under 100 nm of gold and the formation of an interdigitated electrode array (IEA) using a lift-off process.

Biochip surface functionalization

The surface of biochips was then modified for immobilizing the antibody. The chips were first immersed in acetone in a crystallizing dish for 10 min to dissolve away the protective PR layer. The chips were then treated with 1:1 mixture of concentrated methanol and hydrochloric acid for 30 min followed by immersion into boiling distilled water for 30 min. The biochips were allowed to air dry completely. The biochips were then silanized in an anaerobic glove box. The biochips were immersed in a crystallizing dish containing a solution of 2% 3-Mercaptopropytrimethyloxysilane (MTS) (Sigma; St.Louis, MS) for 2 h. The chips were then rinsed in toluene and were allowed to dry completely. After silanization, N-y-maleimidobutyryloxy succinimide ester (GMBS) (Sigma; St.Louis, MA) was chosen as crosslinkers to avoid formation of multi-protein complex. The crosslinking reagent was dissolved in a minimum amount of dimethylformamide (DMF) and then diluted with ethanol to a final concentration of 2 mM. The silanized substrate was treated with crosslinker for 1 hour and washed in phosphate buffered saline (PBS, pH 7.4). After the application of the crosslinker, antibody (Sigma; St.Louis, MA) was immobilized onto the biochip active surface. The biochips were placed in a petri dish, sealed with parafilm and allowed to incubate at 37^{o}C for 1 h. The biochips were then treated with 2 mg/mL bovine serum albumin (BSA)

(Sigma; St.Louis, MA) for 45 min. After incubation, the biochip surface was rinsed with PBS (pH 7.4) and was allowed to air dry (summarized in **Supplementary Fig.2)**.

ACKNOWLEDGMENTS

This work was supported by a research grant from National Science Foundation: NSF EECS-0622056. The authors thank Lurie Nanofabrication Facility at the University of Michigan for the fabrication of biochips. The authors also would like to thank Professor Rita Colwell from University of Maryland, College Park and Professor Gert Cauwenberghs from University of California, San Diego for their critical comments.

AUTHOR CONTRIBUTIONS

Y.L designed and fabricated the FEC biochip and logic gates, performed the verification experiments of "co-detection" principle, and contributed to the planning and writing of the manuscript. E.C.A was a collaborator on the paper and provided all facilities for biological experiments. S.C proposed an original idea of "co-detection" principle as well as supervised the analysis and contributed to the writing of the manuscript.

REFERENCES

1. Draghici, S., Khatri, P., Eklund, A.C., Szallasi, Z., Reliability and reproducibility issues in DNA microarray measurements, *Trends in Genetics*, 22: 101-109 (2005).
2. Marshall, E., Getting the noise out of gene arrays, *Science* 306, 630-631 (2004).

3. Wang, Y., *et al*. HykGene: a hybrid approach for selecting marker genes for phenotype classification using microarray gene expression data, *Bioinformatics* 21, 1530-1537 (2005).

4. Fitch, J.P., Raber, E., Imbro, D. R., Technology challenges in responding to biological or chemical attacks in the civilian sector, *Science* 302, 1350-1354 (2003).

5. Huse, S. M., *et al*. Accuracy and quality of massively parallel DNA pyrosequencing, *Genome Biology* 8, R143 (2007).

6. Noonan, J. P., *et al*. Sequencing and analysis of Neanderthal genomic DNA, *Science* 314, 1113-1118 (2006).

7. Selby, C., Interference in immunoassay, *Ann. Clin.Biochem.* 36, 704-721 (1999).

8. Almog, R., *et al*, Signal amplification in a nanomechanical duffing resonator via stochastic resonance*, Appl.Phys.Lett*. 90, 013508 (2007).

9. Wiesenfeld, K., Moss, F., Stochastic resonance and the benefits of noise: from ice ages to crayfish and SQUIDS, *Nature* 373, 33-36 (1995).

10. Russell, D., Wilkens, L., Moss, F., Use of behavioral stochastic resonance by paddlefish for feeding, *Nature* 402, 219-223 (1999).

11. Liu, Y., Chakrabartty, S., Alocilja, E. C., Fundamental building blocks for molecular bio-wire based forward-error correcting biosensor, *Nanotechnology* 18, 4240107 (2007).

12. Liu, Y., Chakrabartty, S., Factor graph based biomolecular circuit analysis for designing forward error correcting biosensors, *IEEE Transaction on Biomedical Circuits and Systems* 3, 150-159 (2009).

13. Park, S. J., Taton, T. A., Mirkin C.A., Array-based electrical detection of DNA with nanoparticle probes, *Science* 295, 1503-106 (2002).

14. Velev, O. D., Kaler, E. W., In situ assembly of colloidal particles into miniaturized biosensors, *Langmuir* 15, 3693 (1999).

15. Gupta, S, *et al*, Characterization and optimization of gold nanoparticle-based silver-enhanced immunoassays, *Anal. Chem.* 79, 3810-3820 (2007).

16. Shyu R. H., Colloidal gold-based immunochromatographic assay for detection of Ricin, *Toxicon* 40, 255-258 (2002).

17. Liao, K. T., Huang, H. J., Femtomolar immunoassay based on coupling gold nanoparticle enlargement with square wave stripping voltammetry, *Analytica chimica acta* 538, 159-164 (2005).

18. R. Christensen, J. Amer. Statist. Assoc. 95, 2000.

19. Phillippy, A. M., Comprehensive DNA signature discovery and validation, *PLoS Comput Biol* 3(5) (2007).

20. Grant, R. M., AIDS: promote HIV chemoprohylaxis research, don't prevent it, Science 30, 2170-2171 (2005).